

MATHEMATICAL METHOD FOR PREDICTION AEROELASTIC PHENOMENA AND MULTIDISCIPLINARY OPTIMIZATION LIFTING SURFACES OF FLIGHT VEHICLE AT PRELIMINARY STAGE DESIGN

Oleh Havaza¹, Vitalii Sukhov¹

¹ National Technical University of Ukraine “Igor Sikorsky Kyiv Polytechnic Institute”

Kiev, Ukraine

(o.gavaza, v.sukhov)@kpi.ua

Keywords: Aeroelasticity, aeroelastic tailoring, symbolic model, MDO, tensor product model, ROM, concurrent design,

Abstract: Every year, the air transportation market increases the requirements for aircraft performance in order to obtain greater profits. Satisfaction of this requirement is the main purpose for aircraft manufacturer. One of the ways to achieve this purpose is improving the design process by developing and implementing new approaches and tools for modelling different phenomena (in considered case – Aeroelastic phenomena) inherent to flight vehicles.

The purpose of this report is to present a modern mathematical method that allows modelling static and dynamic Aeroelastic Phenomena by a symbolic operation, in contrast to the numerical methods that are widely used today.

The theory of this method based on science analogies approach which allow to present interaction (considering 6 DOF) between aeroelastic forces in analytical formulation, using modern Computer Algebra System tools and as results exclude iteration calculations which inherent inverting and eigenvalue extraction of large dimension matrixes.

Approach of this method based on reduced order modelling principle and main idea is presenting lifting surface (wing, blade, etc.) as a principal scheme which look as parallel, serial and star connection of three types of elements: aerodynamical, elastic and inertial. Each element describes by respective matrixes of parameters with maximum dimension of 6x6 for 6 DOFs (3 translations + 3 rotations).

Analysis is performing by transformation scheme (connection nodes condensation) and finding equivalent matrix of “Aeroelasticity” using recurrent equations for each type of connection (analogical with electrical circuit). Described method was validate by modelling: Wing load distribution, Divergence, Effectiveness of control surface and Flutter.

Finally, gotten Math model describes dependences between design variables and aeroelastic characteristic in explicit symbolic form which allow performs wide fast parametric investigation at preliminary stage design. Additional this model will be useful for structure optimization process using analytical methods and for machine learning and will allow expand using artificial intelligence in aerospace structure design.

1 INTRODUCTION

In the highly competitive landscape of the global aviation industry, airline companies are continuously seeking aircraft with enhanced performance. As fuel prices fluctuate and environmental regulations become more stringent, the necessity for aircraft that can deliver superior performance while minimizing operational costs is paramount. This drive for increased

performance encompasses several factors, including fuel efficiency, payload capacity, range, and overall operational reliability. Equally important is the aspect of safety; aircraft must meet the highest safety standards which is required by aviation government. Therefore, aircraft manufacturers are under immense pressure to innovate and improve their designs to meet these evolving demands while maintaining or exceeding current safety standards.

To achieve these stringent requirements, aircraft manufacturers are increasingly turning to innovative materials and advanced design concepts [1,2]. The use of composite materials, known for their strength and light weight, is becoming more prevalent in the construction of modern aircraft. Additionally, new aircraft layouts, such as braced wings and high aspect ratio designs, are being explored to enhance aerodynamic efficiency and performance [3, 4]. However, these approaches result in increased wing flexibility, posing significant challenges in the design process including Aeroelasticity as important scope which must be considered in preliminary or even better on conceptual stage design [5, 6, 7].

Modern information technologies enable the highly accurate analysis of strength, aerodynamics, and aeroelasticity for well-known flexible aircraft structures, where specific technical solutions have been established, since they based on solving differential equations using various numerical methods such as FEM and Fluid structure interaction (FSI) realized by interchanging data between aerodynamic and structural solvers [8,9]. For these reasons the most known, high accurate tools applicable for final stage design to verification and validation applied decisions.

Consequently, there is a growing demand for the creation of new tools [10] and methodologies based on new paradigms and approaches to predict aircraft characteristics and perform MDO within aeroelastic effects that arise from advanced configurations at conceptual design stage [11]. The primary objective of this paper is to present a cutting-edge approach to the difficult problem of mathematically modeling the aeroelasticity phenomena inherent of atmospheric flight vehicles at the preliminary stage of aircraft design. This approach based on paradigm for modeling aeroelasticity phenomena. This approach is based on ROM [12] and calculation operations performed using tensor forms [13]. In source [14] was used the similar approach with using tensors to modeling flight dynamic of different air vehicle and in sources [15,16,17] tensor product model used for investigation of Aeroservoelasticity scope considering limited Degrees-of-freedom (DOF).

Mentioned works shows that tensor modeling intersects with different disciplines and open wide opportunity to formalization entire aircraft model and incorporates multidisciplinary optimization techniques [18].

Additionally, technique presented in this paper have already been successfully applied to obtain critical speed of wing divergence [19], and was shown ability to perform multidisciplinary optimization in symbolic forms [20], by Lagrange multipliers.

Proposed shift paradigm of analysis from numerical calculation to symbolic operation with applying modern Computer algebra systems (CAS) [21].

The present work is organized as follows. In section 2, described theoretical approach of presented methodology. In section 3 provided general models for analysis aeroelastic phenomena. Finally, the last section summarizes and concludes the article, and suggests research directions for future work.

2 THEORY OF THE METHODOLOGY

2.1 General approach

The main task of aeroelasticity is modeling the interaction of all the above-mentioned forces or their combinations depending on the aeroelastic phenomenon under consideration. Presented method, performs mathematical modeling of aeroelastic phenomena in a visual form using a schematic diagram of the interaction of aeroelastic forces, followed by its transformation and bringing to a certain form depending on the task being solved.

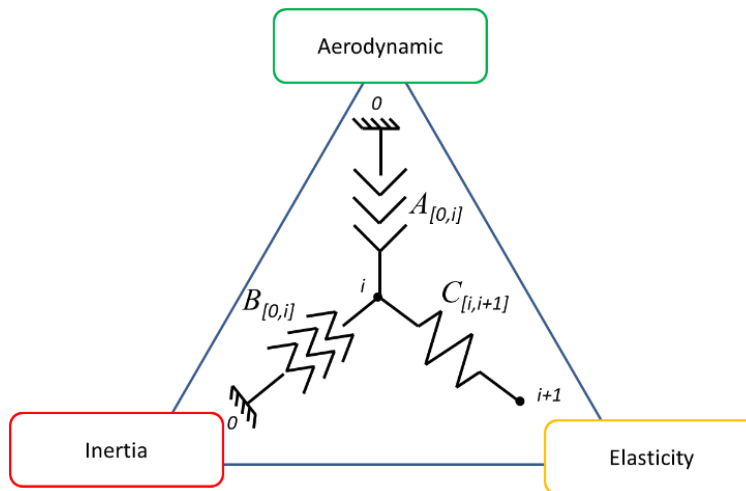


Figure 1: Triangle and “star” of Aeroelasticity

The basis of the method initially developed by Balabanov I.V [22] named as "Nodal condensation method" and use for analysis elastic frames of gyro device in three-dimensional space [23].

Based on the conducted research, the following algorithm for applying this method in the modeling of aeroelastic phenomena has been developed. Consider wing as one of the most important parts of the aircraft which undergoing aeroelastic effects.

It is assumed that wing a regular structure, and it is permitted its division into a series of finite-element sections.

Each section, which is used for the element division, is represented as a node in the analysis diagram, with a corresponding number. Each node serves as a reference point where displacement and the acting or emerging force are subsequently determined.

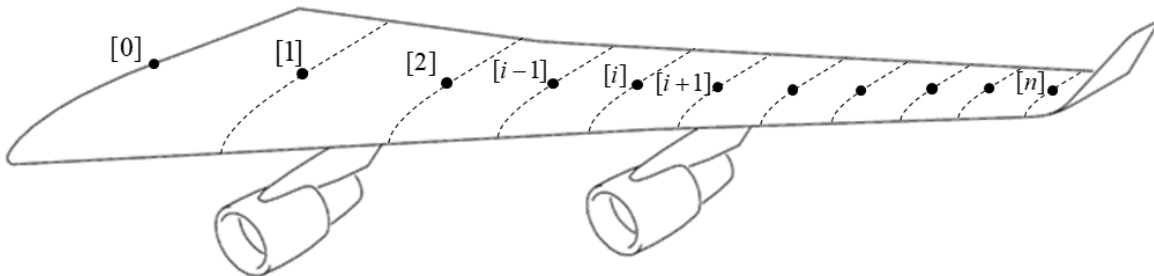


Figure 2: Wing section dividing

Next step is creation of aeroelastic forces interaction scheme by following way.

Each finite element between sections $[i-1]$ and $[i]$ is replaced in the diagram by elements with specific designations according to their nature and impact on the formation of the aeroelastic properties of the entire object. In the general case, each section contains the following three types of elements, which characterize the influence of aeroelastic forces:

- Elastic elements, which account for the emergence of elastic reaction forces and are mathematically described by the stiffness matrix $C_{[i,i+1]}$.
- Inertial elements, which characterize the action of inertia forces and are mathematically described by the inertia matrix $B_{[0,i]}$.
- Aerodynamic elements, which model the influence of aerodynamic forces. This influence is described by the aerodynamic operator $A_{[0,i]}$, also known as the aerodynamic influence matrix or aerodynamic stiffness.

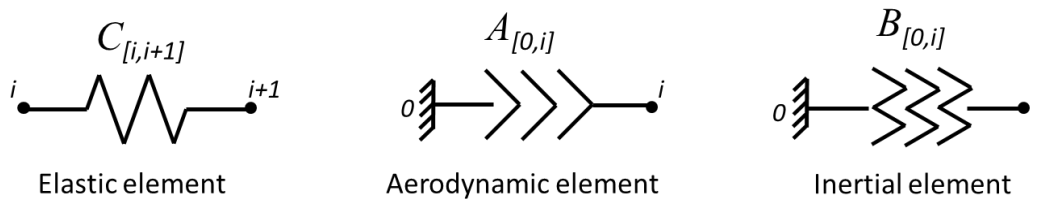


Figure 3: Typical elements using for aeroelasticity modeling

Forces, which are conditionally constant and independent from wing deformation as following examples: weight loads from fuel and structural elements, engine thrust loads and the component of lift force from the wing installation angles of attack. These forces are gathered into a node adjacent to the finite element section and are mathematically expressed as the vector of applied forces $Q_{[i]}$.

Thus, the discrete computational scheme for an idealized wing represents an ordered system consisting of loaded nodes connected to each other by the corresponding inter-node links. The elastic properties are represented as a set of sequentially connected elastic elements, while the aerodynamic and inertial forces are modeled by parallel connection of the respective elements at the nodes, linking them to a notional base. It should be noted that the notional base for the aerodynamic and inertial elements implies that the corresponding forces, unlike the elastic forces, arise outside the structure.

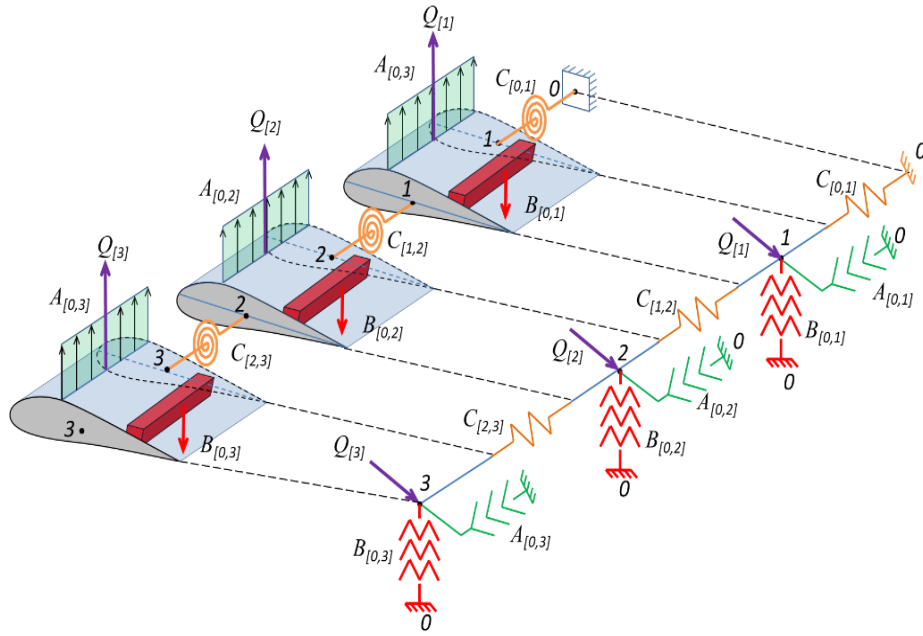


Figure 4: Example of wing dividing for three elements

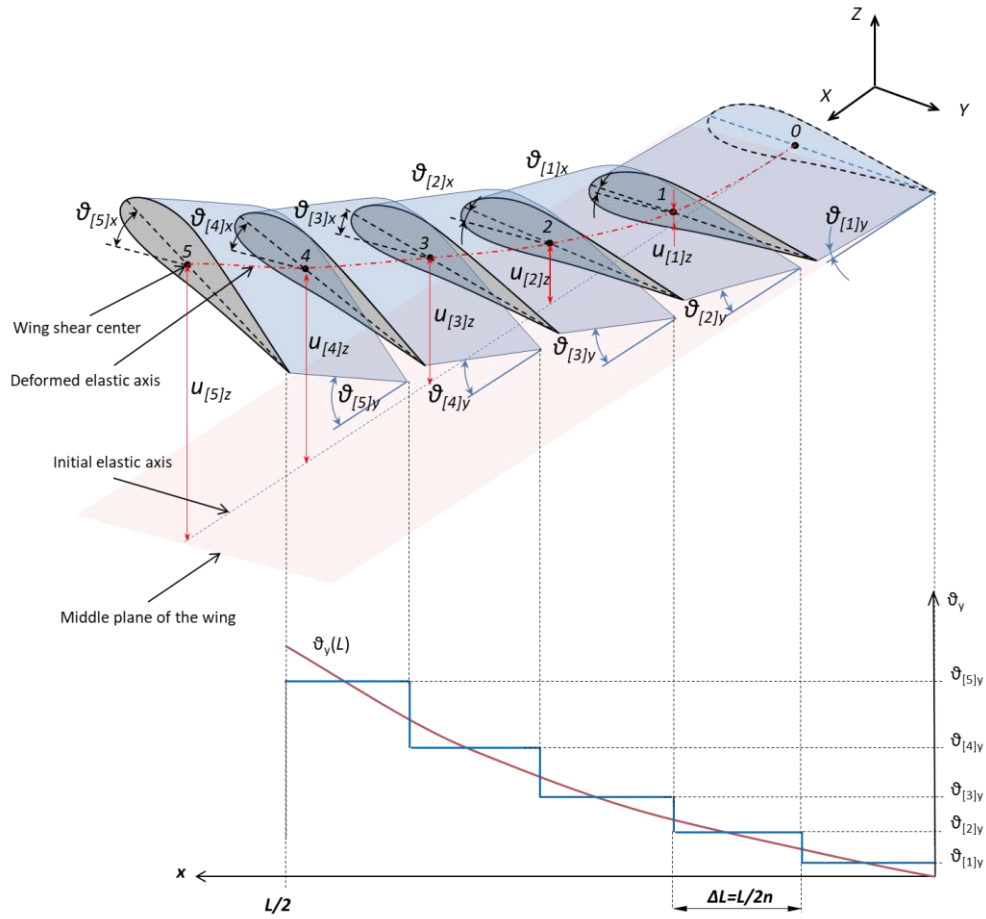


Figure 5: Step approximation of wing deformation.

It is worth noting that the deformation pattern with this representation is stepwise (Figure 5), and the greater the degree of discretization, the more accurately the model corresponds to the real behavior of the elastic wing. On the other hand, with increasing discreteness, the number of variables increases, which in turn leads to the cumbersomeness of the mathematical model. Coming from this, we can conclude that the degree of detail must be selected from the conditions of maintaining a balance between accuracy and the number of design variables, depending on the type of problem being solved and the design stage.

2.2 Mathematical description of the elements of the design scheme

2.2.1 Acting forces and resulting displacements in the node of the base finite element.

At each node of the design scheme, a load can be simultaneously applied and generated, described using vectors of columns of generalized forces.

Let's describe a system of forces and moments acting at a point O_e and defined in the SC $O_e x_e y_e z_e$.

$$Q_{\{e\}[m]}^{(n)} = [P_{\{e\}[m]x}^{(n)} \quad P_{\{e\}[m]y}^{(n)} \quad P_{\{e\}[m]z}^{(n)} \quad M_{\{e\}[m]x}^{(n)} \quad M_{\{e\}[m]y}^{(n)} \quad M_{\{e\}[m]z}^{(n)}]^T \quad (1)$$

The following notation is introduced here:

$P_{\{e\}[m]x}^{(n)}$, $P_{\{e\}[m]y}^{(n)}$, $P_{\{e\}[m]z}^{(n)}$, $M_{\{e\}[m]x}^{(n)}$, $M_{\{e\}[m]y}^{(n)}$, $M_{\{e\}[m]z}^{(n)}$ - components of the column vector acting at m the i th node of the generalized force, describing the projections of force $P_{[m]}^{(n)}$ and moment $M_{[m]}^{(n)}$ onto the corresponding axes of the base coordinate system $O_e x_e y_e z_e$.

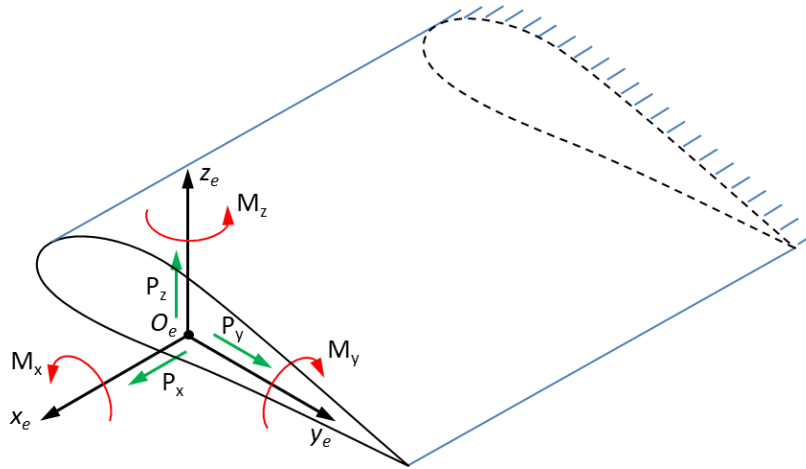


Figure 6: Force vector components

In turn, the movements of the nodes of the design scheme are described using column vectors of generalized movements. For example, the column vector of a generalized node displacement m will look like

$$q_{\{w\}[m]} = [u_{\{w\}[m]x} \quad u_{\{w\}[m]y} \quad u_{\{w\}[m]z} \quad \mathcal{G}_{\{w\}[m]x} \quad \mathcal{G}_{\{w\}[m]y} \quad \mathcal{G}_{\{w\}[m]z}]^T \quad (2)$$

Where:

$u_{\{w\}[m]x}$, $u_{\{w\}[m]y}$, $u_{\{w\}[m]z}$, $\vartheta_{\{w\}[m]x}$, $\vartheta_{\{w\}[m]y}$, $\vartheta_{\{w\}[m]z}$ - components of the column vector of the generalized displacement, describing the projections of the linear $u_{\{w\}[m]}$ and angular $\vartheta_{\{w\}[m]}$ displacement m of the node onto the corresponding axes of the base coordinate system $O_w x_w y_w z_w$.

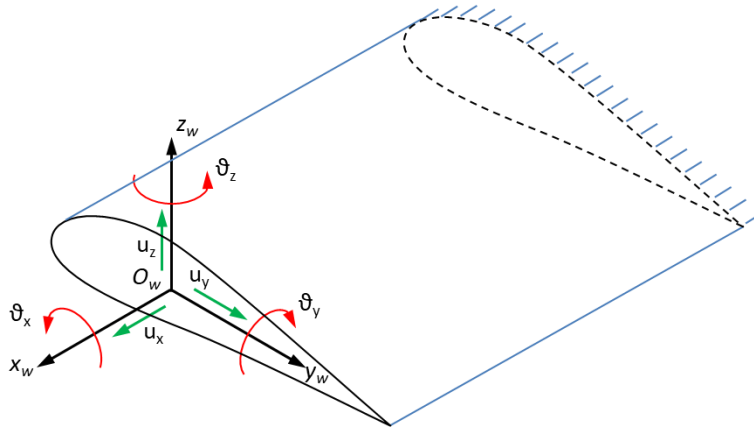


Figure 7: Components of a displacement vector

2.2.2 Mathematical model of restoring elastic forces of a basic finite element.

Since real structures are a spatial elastic system with cross connections between degrees of freedom, for the mathematical representation of stiffness we write a system of equations to determine the elastic reaction forces caused by movement along each of the 6 degrees of freedom. All forces and displacements are defined in the CS $O_c x_c y_c z_c$.

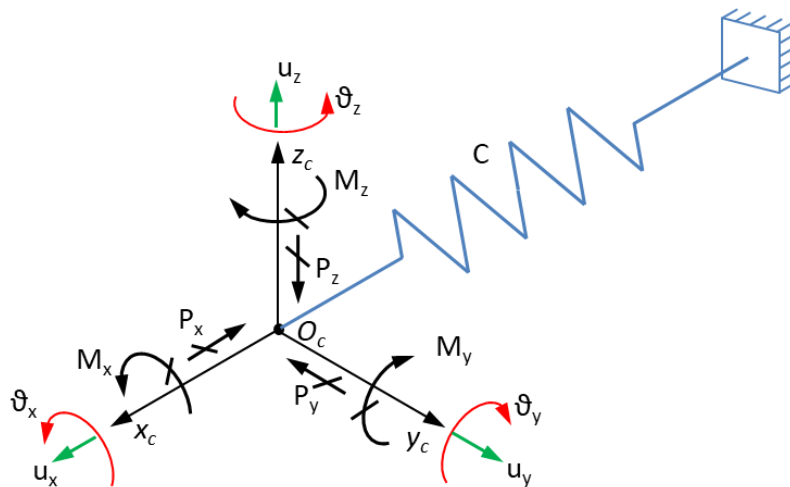


Figure 8: Elastic reactions in a spatial element

$$\begin{cases} P_x = c_{11} \cdot u_x + c_{12} \cdot u_y + c_{13} \cdot u_z + c_{14} \cdot \mathcal{G}_x + c_{15} \cdot \mathcal{G}_y + c_{16} \cdot \mathcal{G}_z \\ P_y = c_{21} \cdot u_x + c_{22} \cdot u_y + c_{23} \cdot u_z + c_{24} \cdot \mathcal{G}_x + c_{25} \cdot \mathcal{G}_y + c_{26} \cdot \mathcal{G}_z \\ P_z = c_{31} \cdot u_x + c_{32} \cdot u_y + c_{33} \cdot u_z + c_{34} \cdot \mathcal{G}_x + c_{35} \cdot \mathcal{G}_y + c_{36} \cdot \mathcal{G}_z \\ M_x = c_{41} \cdot u_x + c_{42} \cdot u_y + c_{43} \cdot u_z + c_{44} \cdot \mathcal{G}_x + c_{45} \cdot \mathcal{G}_y + c_{46} \cdot \mathcal{G}_z \\ M_y = c_{51} \cdot u_x + c_{52} \cdot u_y + c_{53} \cdot u_z + c_{54} \cdot \mathcal{G}_x + c_{55} \cdot \mathcal{G}_y + c_{56} \cdot \mathcal{G}_z \\ M_z = c_{61} \cdot u_x + c_{62} \cdot u_y + c_{63} \cdot u_z + c_{64} \cdot \mathcal{G}_x + c_{65} \cdot \mathcal{G}_y + c_{66} \cdot \mathcal{G}_z \end{cases} \quad (3)$$

For convenience, we introduce the following numbering of the components of the generalized displacement vector q corresponding to linear and angular displacements:

$$q = \begin{bmatrix} u_x & u_y & u_z & \mathcal{G}_x & \mathcal{G}_y & \mathcal{G}_z \end{bmatrix}^T = \begin{bmatrix} q_1 & q_2 & q_3 & q_4 & q_5 & q_6 \end{bmatrix}^T \quad (4)$$

In a similar way, we introduce the numbering of the components of the vector of generalized forces Q corresponding to the acting or emerging forces and moments:

$$Q = \begin{bmatrix} P_x & P_y & P_z & M_x & M_y & M_z \end{bmatrix}^T = \begin{bmatrix} Q_1 & Q_2 & Q_3 & Q_4 & Q_5 & Q_6 \end{bmatrix}^T \quad (5)$$

This system of equations can be written in matrix form:

$$Q = C \cdot q \quad (6)$$

Where

q - Vector of current displacements;

Q - Vector of elastic reaction forces;

C - stiffness matrix (a square matrix of dimensions (6x6), which unambiguously and completely describes the stiffness characteristics of the elastic element under consideration in three-dimensional space.

$$C = \begin{bmatrix} c_{1,1} & c_{1,2} & c_{1,3} & c_{1,4} & c_{1,5} & c_{1,6} \\ c_{2,1} & c_{2,2} & c_{2,3} & c_{2,4} & c_{2,5} & c_{2,6} \\ c_{3,1} & c_{3,2} & c_{3,3} & c_{3,4} & c_{3,5} & c_{3,6} \\ c_{4,1} & c_{4,2} & c_{4,3} & c_{4,4} & c_{4,5} & c_{4,6} \\ c_{5,1} & c_{5,2} & c_{5,3} & c_{5,4} & c_{5,5} & c_{5,6} \\ c_{6,1} & c_{6,2} & c_{6,3} & c_{6,4} & c_{6,5} & c_{6,6} \end{bmatrix} \quad (7)$$

c_{ij} ($i, j = \overline{1,6}$) - elements of the stiffness matrix. Each element c_{ij} is numerically equal to the force arising in the i -th direction under the action of a unit displacement in the j -th direction.

$$c_{ij} = Q_i \Big|_{q_j = 1, Q_k = 0 (\forall k, k \neq j)} \quad (8)$$

2.2.3 Aerodynamic forces of the basic finite element.

Let us introduce the definition of aerodynamic operators by analogy with elastic operators. The aerodynamic forces created by the lifting surface, in turn, depend on a number of parameters, one of which is the derivatives of the aerodynamic coefficients with respect to the angle of attack and angle of slip.

Let's write down the matrix of the most general aerodynamic derivatives defined in a coupled coordinate system $O_A x_A y_A z_A$.

$$\begin{bmatrix} 0 & 0 & 0 & c_x^\alpha & 0 & c_x^\beta \\ 0 & 0 & 0 & 0 & 0 & 0 \\ 0 & 0 & 0 & c_z^\alpha & 0 & c_z^\beta \\ 0 & 0 & 0 & m_x^\alpha & 0 & m_x^\beta \\ 0 & 0 & 0 & m_y^\alpha & 0 & m_y^\beta \\ 0 & 0 & 0 & m_z^\alpha & 0 & m_z^\beta \end{bmatrix} \quad (9)$$

It is also worth noting that the content of the matrix may vary depending on the feasibility of using a particular coefficient in solving a particular problem.

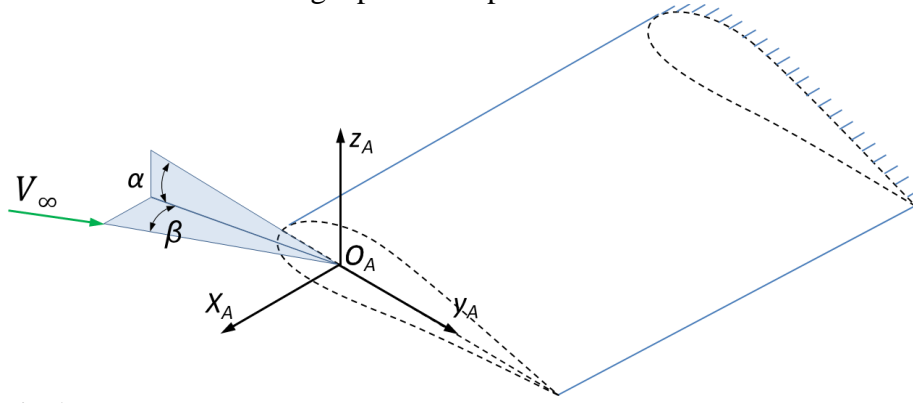


Figure 9: Aerodynamic element

By multiplying the matrix (9) by the magnitude of the dynamic pressure $\frac{\rho \cdot V^2}{2}$ and the characteristic area of the load-bearing surface, S we obtain a matrix of derivatives of aerodynamic forces and moments A (10).

$$A = - \begin{bmatrix} 0 & 0 & 0 & a_{1,4} & 0 & 0 \\ 0 & 0 & 0 & 0 & 0 & a_{1,6} \\ 0 & 0 & 0 & a_{3,4} & 0 & 0 \\ 0 & 0 & 0 & 0 & 0 & a_{4,6} \\ 0 & 0 & 0 & a_{5,4} & 0 & 0 \\ 0 & 0 & 0 & 0 & 0 & a_{6,6} \end{bmatrix} = - \begin{bmatrix} 0 & 0 & 0 & c_x^\alpha & 0 & 0 \\ 0 & 0 & 0 & 0 & 0 & c_y^\beta \\ 0 & 0 & 0 & c_z^\alpha & 0 & 0 \\ 0 & 0 & 0 & 0 & 0 & m_x^\beta \\ 0 & 0 & 0 & m_y^\alpha & 0 & 0 \\ 0 & 0 & 0 & 0 & 0 & m_z^\beta \end{bmatrix} \cdot \frac{\rho \cdot V^2}{2} \cdot S \quad (10)$$

Matrix $A = [a_{i,j}] (i, j = \overline{1,6})$ size 6x6 is a second-rank tensor, which in the general case describes the aerodynamic effect on the elastic wing. It is worth noting that the minus sign (-) in front of the matrix components is indicated for the correct application of the rules of mathematical transformation of the structural diagram.

$a_{ij} (i, j = \overline{1,6})$ - elements of the aerodynamic influence matrix. Each element a_{ij} is numerically equal to the increase in aerodynamic force or moment in the i -th direction with a unit change in the aerodynamic angle relative to the j -th direction.

2.2.4 Generalized inertial forces of the basic finite element.

For convenience, we assume that the axes of the base local coordinate system $O_B x_B y_B z_B$ coincide with the main central axes of inertia i of the i -th finite element section of the wing.

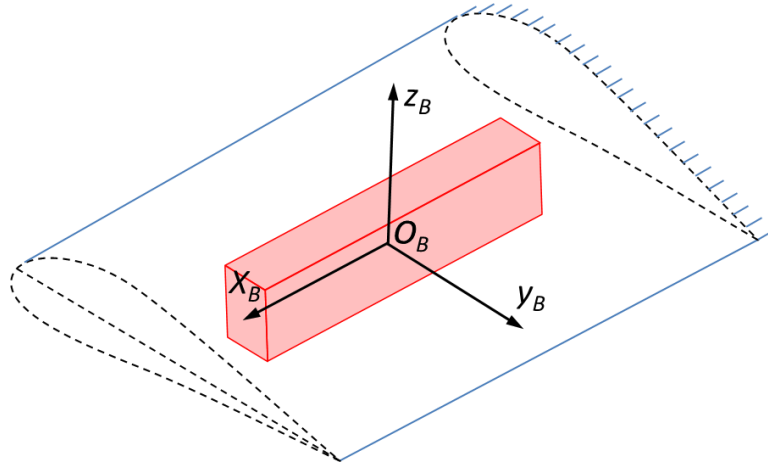


Figure 10: Inertial element

Then the inertia matrix B written in operator form, when defined in the base coordinate system $O_B x_B y_B z_B$, will have the corresponding diagonal form:

$$B = - \begin{bmatrix} m \cdot p^2 & 0 & 0 & 0 & 0 & 0 \\ 0 & m \cdot p^2 & 0 & 0 & 0 & 0 \\ 0 & 0 & m \cdot p^2 & 0 & 0 & 0 \\ 0 & 0 & 0 & J_{xx} \cdot p^2 & 0 & 0 \\ 0 & 0 & 0 & 0 & J_{yy} \cdot p^2 & 0 \\ 0 & 0 & 0 & 0 & 0 & J_{zz} \cdot p^2 \end{bmatrix} \quad (11)$$

m and J_{xx} , J_{yy} , J_{zz} - mass and corresponding principal central moments of inertia i -th final element; $p \equiv \frac{d}{dt}$ - differentiation operator.

Matrix $B = [b_{i,j}] (i, j = \overline{1,6})$ size 6x6 is a tensor rank of two, which in the general case describes the influence of inertial forces when modeling the phenomena of dynamic aeroelasticity. It is also worth noting that the minus sign (-) in front of the matrix components (as well as for the matrix A

) is indicated for the convenience of a mathematical description of the rules for transforming the block diagram.

b_{ij} ($i, j = \overline{1,6}$) - elements of the inertia matrix. Each element $b_{ij} \cdot p^2$ is numerically equal to the increase in inertial force or moment in the i -th direction with unit acceleration relative to the j -th direction.

2.3 Coordinate systems

Since when studying the wing we are dealing with a spatial system, and initially the parameters of each component of the structural diagram are given relative to its own local coordinate system, the main condition for a correct mathematical description of the unit under study is to bring the design diagram to a single reference system, by redefining mathematical operators from local coordinate systems into a single global coordinate system using formulas (15) - (19).

2.3.1 Local coordinate systems

Depending on the choice of coordinate system (CS), matrix operators describing the properties of aeroelastic forces will change not only the numerical values of their elements, but also the structure of the matrix itself.

To organize the design scheme in all similar finite element sections, local basic coordinate systems (Figure 11) are introduced according to the following principle:

- for the wing profile elements that generate lift, coordinate systems are introduced $O_a x_a y_a z_a$, the origins O_a of which lie at the aerodynamic center. $O_a x_a y_a z_a$.
- for the elastic elements of the wing, coordinate systems are introduced $O_c x_c y_c z_c$, the origins O_c of which lie in the corresponding centers of rigidity. $O_c x_c y_c z_c$.
- for the inertial elements of the wing, coordinate systems are introduced $O_b x_b y_b z_b$, the origins O_b of which lie in the corresponding centers of mass.

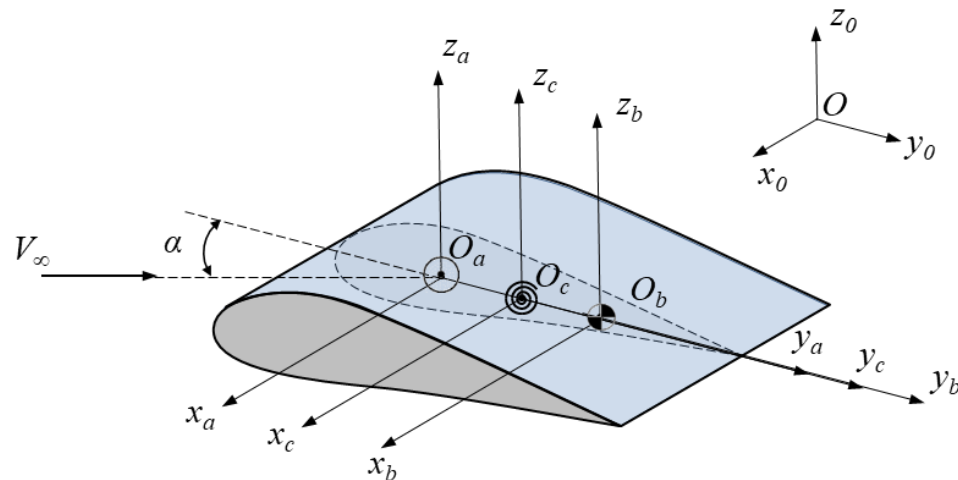


Figure 11: Coordinate systems of the basic finite element

2.3.2 Formation of a transition matrix between coordinate systems

The position of characteristic points (centers of pressure, stiffness, mass and the point of application of the force vector), coinciding with the origin of the local coordinate system (in the general case $O_w x_w y_w z_w$), relative to the global coordinate system $O_0 x_0 y_0 z_0$ is characterized by the coordinates of the origin of the global coordinate system $O_0 x_0 y_0 z_0$ relative to the center of the local coordinate system $O_{c,b,a,i} - r_{x_0}^{(c,b,a,i)}$, $r_{y_0}^{(c,b,a,i)}$ and $r_{z_0}^{(c,b,a,i)}$

In turn, these parameters form an skew-symmetric transition matrix between coordinate systems $O_w x_w y_w z_w$ and $O_0 x_0 y_0 z_0$ with linear displacement, which has the following structure:

$$R_{0w}^\vee = \begin{bmatrix} 0 & -r_{z_0}^{(w)} & r_{y_0}^{(w)} \\ r_{z_0}^{(w)} & 0 & -r_{x_0}^{(w)} \\ -r_{y_0}^{(w)} & r_{x_0}^{(w)} & 0 \end{bmatrix} \quad (12)$$

The angular position of the axes of the local coordinate system $O_w x_w y_w z_w$ relative to the global coordinate system $O_0 x_0 y_0 z_0$ will be characterized by the matrix of direction cosines D_{0w}

$$D_{0w} = \begin{bmatrix} \cos(\hat{x}_0 \hat{x}_w) & \cos(\hat{x}_0 \hat{y}_w) & \cos(\hat{x}_0 \hat{z}_w) \\ \cos(\hat{y}_0 \hat{x}_w) & \cos(\hat{y}_0 \hat{y}_w) & \cos(\hat{y}_0 \hat{z}_w) \\ \cos(\hat{z}_0 \hat{x}_w) & \cos(\hat{z}_0 \hat{y}_w) & \cos(\hat{z}_0 \hat{z}_w) \end{bmatrix} \quad (13)$$

where the elements of the matrix are the cosines of the angles between the corresponding axes of the local ($O_w x_w y_w z_w$) and global ($O_0 x_0 y_0 z_0$) coordinate systems.

The skew-symmetric matrix R_{0w}^\vee and the matrix of direction cosines D_{0w} form a coordinate transformation matrix Λ_{0w} that allows the transition from the local base coordinate system ($O_w x_w y_w z_w$) to the global one ($O_0 x_0 y_0 z_0$),

$$\Lambda_{0w} = \begin{bmatrix} D_{0w} & O_{3,3} \\ R_{0w}^\vee D_{0w} & D_{0w} \end{bmatrix} \quad (14),$$

where $O_{3,3}$ is a zero matrix of size (3x3).

Then the determination of the vector of generalized forces in the new coordinate system $O_0 x_0 y_0 z_0$ is carried out according to the following formula:

$$Q_{\{0\}[m]}^{(n)} = \Lambda_{0e} \cdot Q_{\{e\}[m]}^{(n)} \quad (15)$$

- the superscript (n) indicates the number of this generalized force

- in subscripts $\{e\}$ and $[m]$ respectively indicates the number of the base coordinate system $O_e x_e y_e z_e$ in which this generalized force is defined and the number of the node in which this generalized force acts.

It should also be noted that the generalized movements of nodes $q_{\{0\}[s]}$ ($s = \overline{1, n}$) The main system is defined in a global coordinate system $O_0 x_0 y_0 z_0$. In this case, the generalized

displacement m of the n th node $q_{\{0\}[m]}$ and $q_{\{w\}[m]}$, defined in the global $O_0x_0y_0z_0$ and local $O_wx_wy_wz_w$ coordinate systems, are related by the following expression:

$$q_{\{w\}[m]} = \Lambda_{0w}^T \cdot q_{\{0\}[m]} \quad (16)$$

For a stiffness matrix defined in the local coordinate system $O_cx_cy_cz_c$, $C_{\{c\}[n,m]}^{(k)}$ which describes the properties of k the n th elastic element located between n the n th and m th nodes, the transition to the global coordinate system $O_0x_0y_0z_0$ is carried out in accordance with the following formula:

$$C_{\{0\}[n,m]}^{(k)} = \Lambda_{0c} \cdot C_{\{c\}[n,m]}^{(k)} \cdot \Lambda_{0c}^T \quad (17)$$

where Λ_{0c} is the coordinate transformation matrix, described by the expressions (12)- (14).

By analogy with the stiffness matrices, the determination of the matrices of aerodynamic influence and inertia in the global coordinate system is carried out using the formulas (18) and (19).

For the aerodynamic influence matrix:

$$A_{\{0\}[0,m]}^{(k)} = \Lambda_{0a} \cdot A_{\{a\}[0,m]}^{(k)} \cdot \Lambda_{0a}^T \quad (18)$$

For the inertia matrix:

$$B_{\{0\}[0,m]}^{(k)} = \Lambda_{0b} \cdot B_{\{b\}[0,m]}^{(k)} \cdot \Lambda_{0b}^T \quad (19)$$

2.4 Analysis of the structure of the design scheme and its recurrent transformation.

2.4.1 General description

The essence of presented method is the sequential transformation of the main system into equivalent systems with fewer count of nodes. To do this, it is necessary to determine the main system that models the interaction of all structural elements and generalized forces, by bringing all components of the structural diagram to a single frame of reference.

Consider the basic finite element shown in Figure 12. The generalized finite element corresponds to a basic fragment of the design scheme, consisting of elastic, aerodynamic and inertial elements (described by matrices C , A and B), connecting i the node, respectively, with the previous ($i-1$) node, or with a general ground, and a vector of generalized forces $Q_{[i]}$.

Based on the principle of scientific analogies, it is possible to draw a parallel of similarities between the presented generalized fragment of the design diagram and the circuit diagram of the electrical circuit. The principal interaction scheme circuit as a whole is subjected to similar methods of analysis as when calculating an electrical circuit by transforming the circuit diagram, excluding nodes and finding equivalent resistances.

The proof of the use of this approach was used earlier in the source [23] to calculate spatial elastic systems using the example of an elastic suspension of a gyroscope. This method is called the Nodal Condensation Method (NCM), the essence of which is the sequential transformation of the main system into equivalent elastic systems with fewer nodes. In general, NCM serves as a theoretical basis for current method. The main distinctive feature is the presence of different types (elastic, aerodynamic, inertial) structural elements that make up the design scheme.

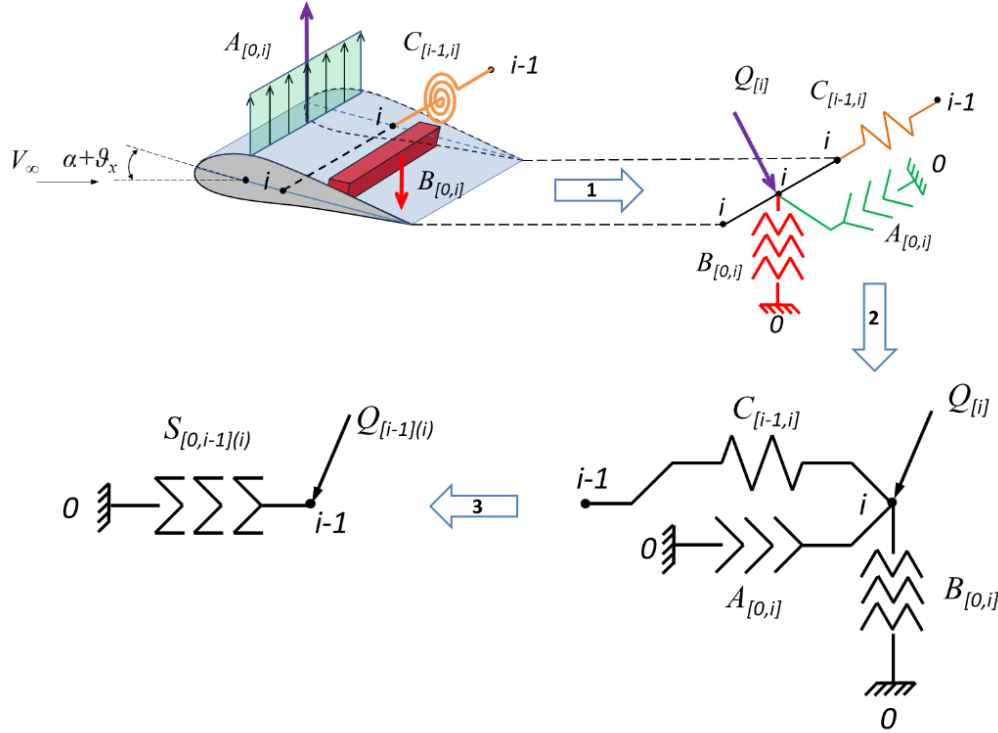


Figure 12: Transformation of the structural diagram based on single section which undergoing elastic, aerodynamic and inertial forces.

It is obvious that the element $B_{[0,i]}$ and $A_{[0,i]}$ are connected in parallel and element $C_{[i-1,i]}$ with serial connection, and the equivalent inter-node connection after transforming the circuit, by analogy with the expression, is determined by the following equation:

$$S_{[0,i-1]} = ((B_{[0,i]} + A_{[0,i]})^{-1} + C_{[i-1,i]}^{-1})^{-1} \quad (20)$$

Then the generalized displacement of node is defined as:

$$q_{[i-1]} = S_{[0,i-1]}^{-1} \cdot Q_{[i-1](i)} \quad (21)$$

2.4.2 Recurrent transformation of a structural diagram with many nodes.

The recurrent transformation of the original system is a recalculation of the generalized matrices of internodal connections and nodal loads obtained by sequentially transforming the main system into equivalent systems with less count of nodes. Let us consider the most common structural diagram of the “star-delta” type for all cases (Figure 13). Then, during its transformation, which consists of eliminating l the l -th node, the generalized matrix $S_{\{0\}[k,m](l)}$ and the node load $Q_{\{0\}[k](l)}$ are determined by the following recurrent formulas:

$$S_{\{0\}[k,m](l)} = S_{\{0\}[k,m]} + S_{\{0\}[k,l]} (S_{\{0\}[l]})^{-1} S_{\{0\}[l,m]} \quad (22)$$

$$Q_{\{0\}[k](l)} = Q_{\{0\}[k]} + S_{\{0\}[k,l]} (S_{\{0\}[l]})^{-1} Q_{\{0\}[l]} \quad (23)$$

where $S_{\{0\}[l]}$ is the sum of the matrices of all internodal connections directly adjacent to l -th node.

$$S_{\{0\}[l]} = \sum_{(\forall s)} S_{\{0\}[l,s]} \quad (24)$$

Here, when denoting generalized matrices $S_{\{0\}[k,m](l)}$ and nodal forces $Q_{\{0\}[k](l)}$ in the transformed system in lower indices after curly and square brackets containing the corresponding data (clause 2.3.2), an index is introduced in parentheses indicating the numbers of all nodes excluded in the transformed system under consideration.

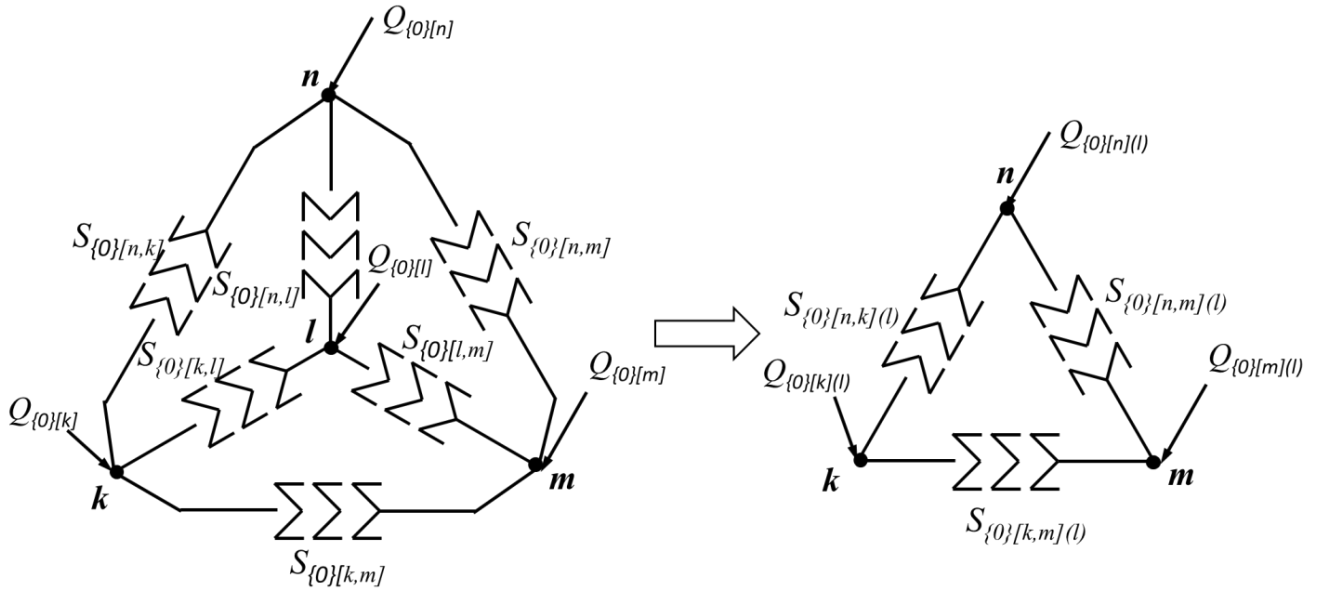


Figure 13: Transformation of the main system

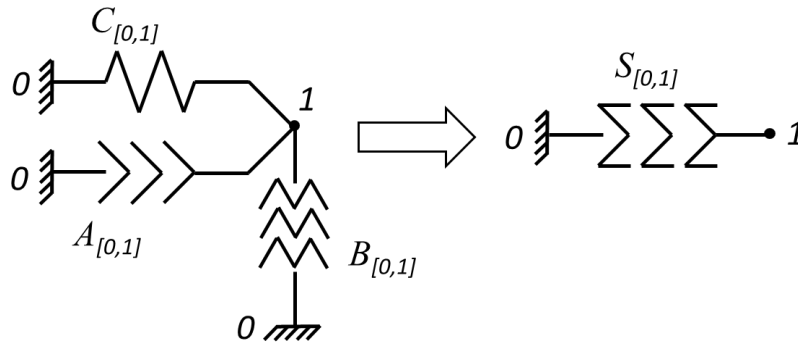


Figure 14: Parallel connection of aeroelastic elements

Accordingly, based on the equation (22), the expression for determining the equivalent inter-node connection for a parallel connection has the following form

$$S_{[0,1]} = C_{[0,1]} + A_{[0,1]} + B_{[0,1]} \tag{25}$$

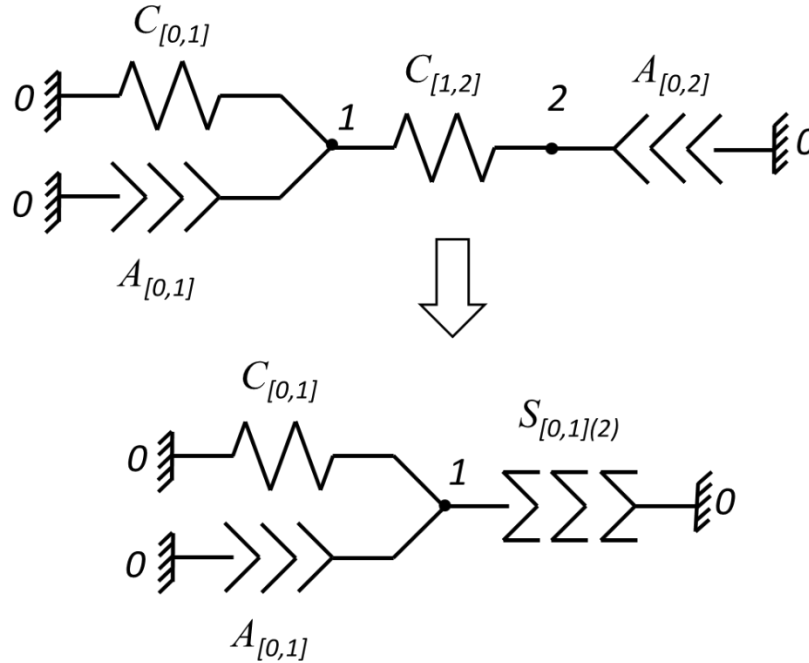


Figure 15: Series connection of aeroelastic elements

During the transformation, which consists of excluding a node 2 from the section of the diagram where elements $C_{[1,2]}$ and are connected in series $A_{[0,2]}$, the expression for determining the equivalent elastic connection has the following form

$$S_{[0,1](2)} = (C_{[1,2]}^{-1} + A_{[0,2]}^{-1})^{-1} \quad (26)$$

To avoid the singularity of the matrix $A_{[0,2]}$ when inverting it, let's rewrite the expression (26) in the following form:

$$S_{[0,1](2)} = C_{[1,2]} \cdot (C_{[1,2]} + A_{[0,2]})^{-1} \cdot A_{[0,2]} \quad (27)$$

3 GENERALIZED MODELS FOR SOLVING AEROELASTICITY PROBLEMS

3.1 Wing divergence

To model the phenomena of static aeroelasticity, only elastic and aerodynamic forces are taken into account (Figure 16). Based on this, to determine the critical divergence speed, we present a structural diagram consisting only of elastic and aerodynamic elements Figure 16, which are described by matrices $C_{(0)}$ and $A_{(0)}$ defined in the global coordinate system $Ox_0y_0z_0$. It is also worth noting that to model this phenomenon of aeroelasticity, nodal forces are excluded from the scheme, since the phenomenon of divergence does not depend on the initial conditions.

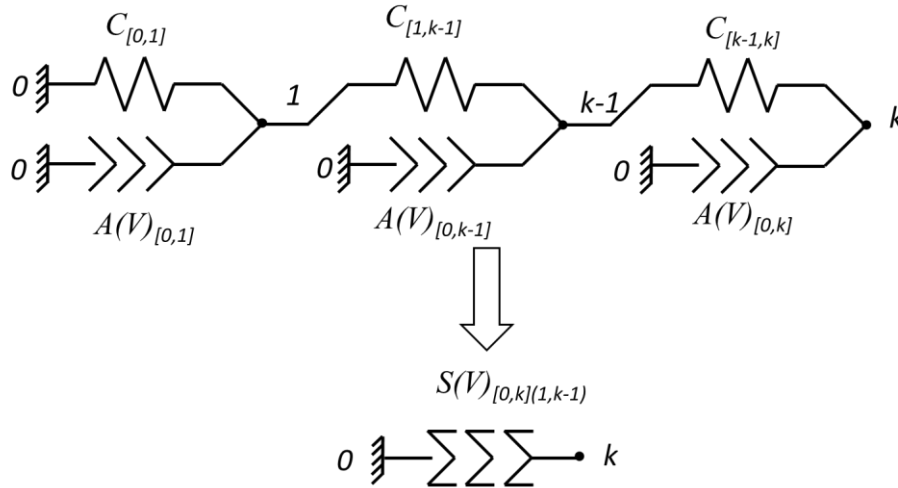


Figure 16: Principal scheme for wing divergence analysis

To determine the parameters of the critical divergence speed, it is necessary to transform the structural diagram by eliminating nodes, with the remaining node k acting as a characteristic point, and the equivalent internodal connection described by the aeroelasticity matrix $S_{[0,k](1,k-1)}$ determines the state of the system (wing) and is expressed by the following formula:

$$S(V)_{[0,k](1,k-1)} = (((C_{[0,1]} + A(V)_{[0,1]})^{-1} + C_{[1,k-1]}^{-1})^{-1} + A(V)_{[0,k-1]}^{-1} + C_{[k-1,k]}^{-1}) + A(V)_{[0,k]} \quad (28)$$

Since, according to the expression, (10) the aerodynamic operators A , and as a consequence, S are functions of the oncoming flow velocity V_∞ , then with an increase in this speed, a moment may occur ~~in the state of the system~~ at which the determinant of the matrix $S_{[0,k](1,k-1)}$ will be equal to zero. The magnitude of this speed is critical.

$$\det S(V_{kp})_{[0,k](1,k-1)} = 0 \quad (29)$$

The expression (29) is the condition for the occurrence of wing divergence. Mathematically, this is explained by the fact that, according to the formula (39) provided (29), the generalized movement of the node k tends to infinity at the slightest load, which is what characterizes the phenomenon of divergence of the load-bearing surface (wing).

$$q_{[k]} = S_{[0,k](1,k-1)}^{-1} \cdot Q_{[k](1,k-1)} \quad (30)$$

It is also worth noting that the choice of a characteristic node to which the equivalent system is reduced does not affect the calculation result.

Examples of a generalized calculation of the critical speed of wing divergence are described in the works [19].

3.2 Deformation of the aerodynamic surface undergoing by air loads

Another possibility of using presented method is to determine the elastic deformation of the wing. Let's consider this problem as determining the parameters of the steady state of the system, without taking into account the parameters of this time domain process. With this approach, we refer the problem to the field of static aeroelasticity.

Below is a generalized model for determining the wing deformation angles at the existing geometric wing twist. Geometric twist is expressed by a vector of values of the installation angles φ_i of each section, specified in the global coordinate system. The aerodynamic load arising due to twist (without taking into account wing deformation) is defined as:

$$Q_{[i]} = A_{[0,i]} \cdot \varphi_i \quad (31)$$

The principal scheme for a 4-th element system is shown in Figure 17

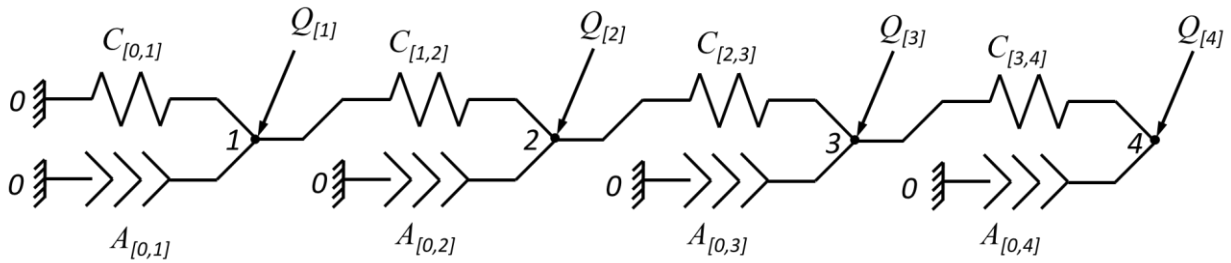


Figure 17: Principal scheme for static aeroelasticity analysis

For calculations, the principal scheme is transformed in such a way that only one node remains. The equivalent internodal connection $S_{[0,i]}$, obtained after transforming the diagram, describes the behavior of node i under load depending on the aerodynamic and stiffness parameters of the entire wing.

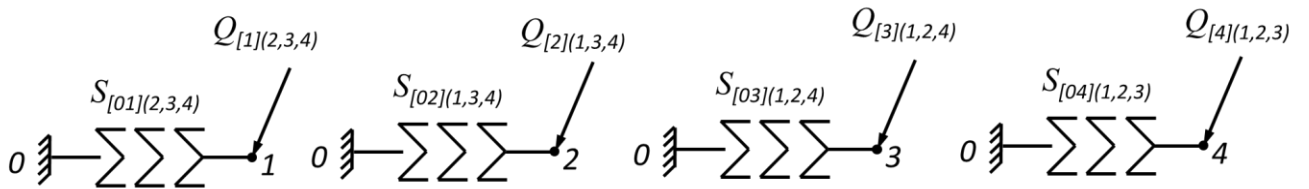


Figure 18: Principal scheme condensation for each node

Obviously, the number of expressions depends on the degree of discretization and is equal to the number of circuit nodes (or sections of the wing span along the span). Expressions describing the equivalent stiffness at each node for a four-element circuit are defined as:

$$S_{01(2,3,4)} = (((((C_{34}^{-1} + A_{04}^{-1})^{-1} + A_{03})^{-1} + C_{23}^{-1})^{-1} + A_{02})^{-1} + C_{12}^{-1})^{-1} + A_{01} + C_{01} \quad (32)$$

$$S_{02(1,3,4)} = [((C_{01} + A_{01})^{-1} + C_{12}^{-1})^{-1} + A_{02}] + [(((C_{34}^{-1} + A_{04}^{-1})^{-1} + A_{03})^{-1} + C_{23}^{-1})^{-1}] \quad (33)$$

$$S_{03(1,2,4)} = [(((C_{01} + A_{01})^{-1} + C_{12}^{-1})^{-1} + A_{02})^{-1} + C_{23}^{-1}) + A_{03}] + [(C_{34}^{-1} + A_{04}^{-1})^{-1}] \quad (34)$$

$$S_{04(1,2,3)} = ((((((C_{01} + A_{01})^{-1} + C_{12}^{-1})^{-1} + A_{02})^{-1} + C_{23}^{-1})^{-1} + A_{03})^{-1} + C_{34}^{-1})^{-1} + A_{04} \quad (35)$$

The next step for the adequacy of the mathematical model is to determine the equivalent force acting in a characteristic node with the rest excluded. The expression for the desired force is determined in accordance with the expression (23).

The physical meaning of this expression is to describe the influence of aerodynamic, stiffness and geometric (distribution of twist angles along the span) parameters of the wing on the magnitude of the resulting aerodynamic force in a certain section of the wing. It is obvious that, just as for the equivalent stiffness, the number of expressions for the equivalent force corresponds to the number of nodes.

$$Q_{1(2,3,4)} = Q_1 + K_{21} \cdot Q_2 + K_{21} \cdot K_{32} \cdot Q_3 + K_{21} \cdot K_{32} \cdot K_{43} \cdot Q_4 \quad (36)$$

$$Q_{2(1,3,4)} = K_{12} \cdot Q_1 + Q_2 + K_{32} \cdot Q_3 + K_{32} \cdot K_{43} \cdot Q_4 \quad (37)$$

$$Q_{3(1,2,4)} = K_{23} \cdot K_{12} \cdot Q_1 + K_{23} \cdot Q_2 + Q_3 + K_{43} \cdot Q_4 \quad (38)$$

$$Q_{4(1,2,3)} = K_{34} \cdot K_{23} \cdot K_{12} \cdot Q_1 + K_{34} \cdot K_{23} \cdot Q_2 + K_{34} \cdot Q_3 + Q_4 \quad (39)$$

Where are the matrices K used for reduce the equations of formulas and for the case of a 4-element wing are defined as:

$$K_{12} = C_{12}(C_{01} + A_{01} + C_{12})^{-1} \quad (40)$$

$$K_{21} = C_{12}(C_{12} + A_{02} + (((C_{34}^{-1} + A_{04}^{-1})^{-1} + A_{03})^{-1} + C_{23}^{-1})^{-1})^{-1} \quad (41)$$

$$K_{23} = C_{23}(C_{23} + ((C_{01} + A_{01})^{-1} + C_{12}^{-1})^{-1} + A_{02})^{-1} \quad (42)$$

$$K_{32} = C_{23}(C_{23} + A_{03} + (C_{34}^{-1} + A_{04}^{-1})^{-1})^{-1} \quad (43)$$

$$K_{34} = C_{34}(C_{34}(((C_{01} + A_{01})^{-1} + C_{12}^{-1})^{-1} + C_{23}^{-1})^{-1} + A_{02})^{-1} + C_{23}^{-1})^{-1} + A_{03})^{-1} \quad (44)$$

$$K_{43} = C_{34}(C_{34} + A_{04})^{-1} \quad (45)$$

The displacement of each node during wing deformation is defined as:

$$q_1 = S_{01(2,3,4)}^{-1} \cdot Q_{1(2,3,4)} \quad (46)$$

$$q_2 = S_{02(1,3,4)}^{-1} \cdot Q_{2(1,3,4)} \quad (47)$$

$$q_3 = S_{03(1,2,4)}^{-1} \cdot Q_{3(1,2,4)} \quad (48)$$

$$q_4 = S_{04(1,2,3)}^{-1} \cdot Q_{4(1,2,3)} \quad (49)$$

Now let's express the force acting in the i -th node in the form $Q_i = A_{0i} \cdot \varphi_i$, where is φ_i the angle of geometric twist on the i -th section of the wing and write down the (46) – (49) equations in expanded form as following:

$$q_1 = S_{01}^{-1} \cdot A_{01} \cdot \varphi_1 + S_{01}^{-1} \cdot K_{21} \cdot A_{02} \cdot \varphi_2 + S_{01}^{-1} \cdot K_{21} \cdot K_{32} \cdot A_{03} \cdot \varphi_3 + S_{01}^{-1} \cdot K_{21} \cdot K_{32} \cdot K_{43} \cdot A_{04} \cdot \varphi_4 \quad (50)$$

$$q_2 = S_{02}^{-1} \cdot K_{12} \cdot A_{01} \cdot \varphi_1 + S_{02}^{-1} \cdot A_{02} \cdot \varphi_2 + S_{02}^{-1} \cdot K_{32} \cdot A_{03} \cdot \varphi_3 + S_{01}^{-1} \cdot K_{32} \cdot K_{43} \cdot A_{04} \cdot \varphi_4 \quad (51)$$

$$q_3 = S_{03}^{-1} \cdot K_{23} \cdot K_{12} \cdot A_{01} \cdot \varphi_1 + S_{03}^{-1} \cdot K_{23} \cdot A_{02} \cdot \varphi_2 + S_{03}^{-1} \cdot A_{03} \cdot \varphi_3 + S_{03}^{-1} \cdot K_{43} \cdot A_{04} \cdot \varphi_4 \quad (52)$$

$$q_4 = S_{04}^{-1} \cdot K_{34} \cdot K_{23} \cdot K_{12} \cdot A_{01} \cdot \varphi_1 + S_{04}^{-1} \cdot K_{34} \cdot K_{23} \cdot A_{02} \cdot \varphi_2 + S_{04}^{-1} \cdot A_{03} \cdot K_{34} \cdot A_{03} \cdot \varphi_3 + S_{04}^{-1} \cdot A_{04} \cdot \varphi_4 \quad (53)$$

These matrix equations are integral mathematical models describing the movements of a certain section of the aerodynamic surface in the air flow, and are functions of the aerodynamic and elastic characteristics of the wing.

3.3 Efficiency of the control surface of an elastic wing

To study the basic physical laws affecting the effectiveness of ailerons on an elastic wing, consider a three-element, one-dimensional (twist only) idealized wing model presented in

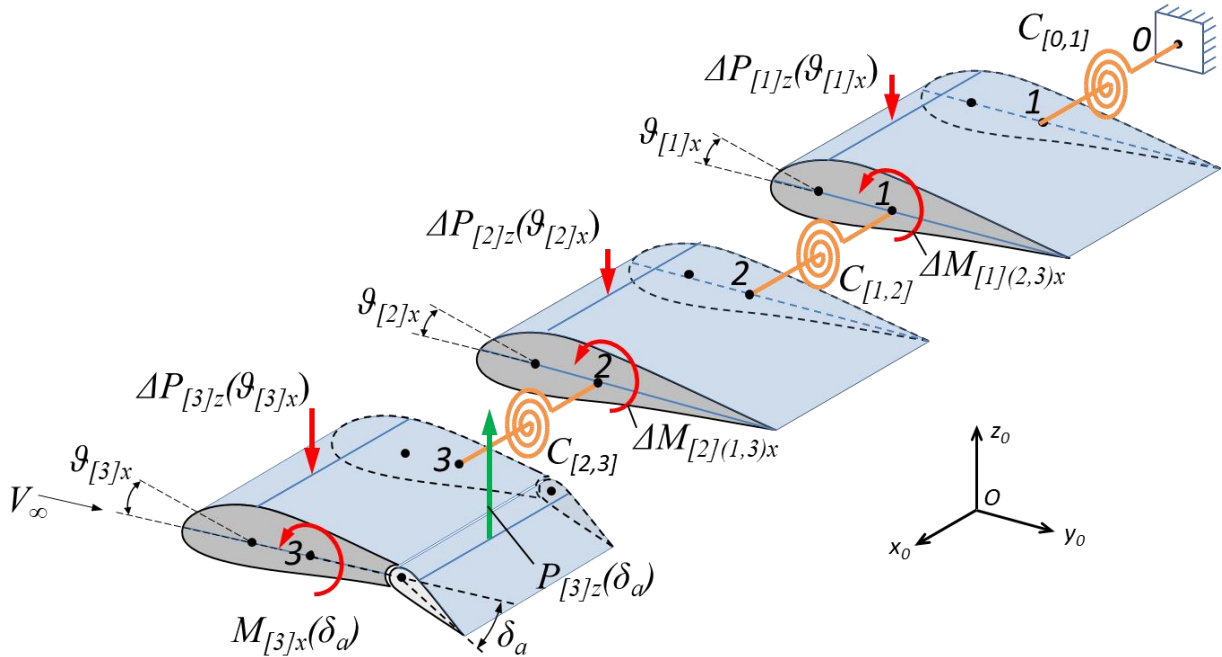


Figure 19: Idealization of the wing for the aileron reverse speed definition

The aileron has the ability to deviate by an angle δ_a from the static equilibrium position of the wing. If we now assume that the wing compartment is rigidly fixed, then when the aileron is deflected downward, the lift force increases, and the resulting increase in lift force is applied behind the line of wing foci.

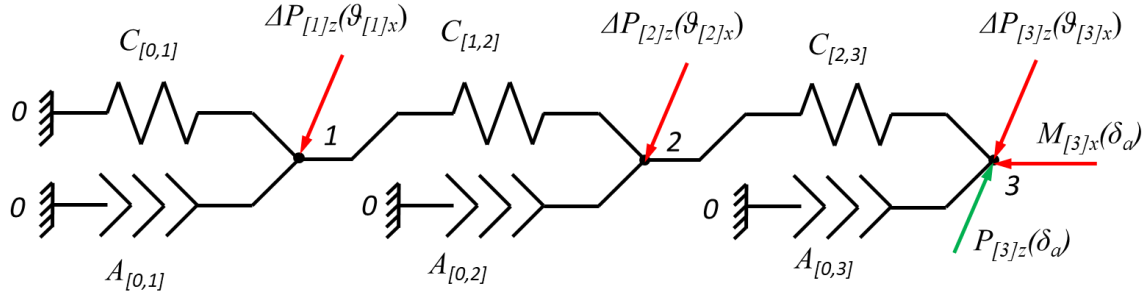


Figure 20: Principal scheme according to the aileron reverse speed definition

If now the additional force $P_{[3]z}(\delta_a)$ is moved to the focus, then at the same time it is necessary to apply a negative aerodynamic moment $M_{[3]x}(\delta_a)$, tending to rotate the elastic wing in the direction of decreasing the angle of attack by the deformation angle $\vartheta_{[i]x}$, determined in each i section. As a result, we obtain a decrease in the total increase in lift force ΔP_z^Σ on the elastic wing console. The total increase in the lifting force of the console will be determined by the formula:

$$\Delta P_z^\Sigma = P_{[3]z}(\delta_a) - \Delta P_{[3]z}(\vartheta_{[3]x}) - \Delta P_{[2]z}(\vartheta_{[2]x}) - \Delta P_{[1]z}(\vartheta_{[1]x}) \quad (54)$$

The moment $M_{[3]x}(\delta_a)$ is proportional to the square of the flow velocity, while the elastic restoring moment does not depend on the speed. Consequently, with an increase in flow speed, the effectiveness of the aileron in terms of the increase in lift force decreases and at the so-called critical speed of aileron reverse, their effectiveness is zero, i.e., the total lift force remains unchanged.

$$\Delta P_z^\Sigma = 0 \quad (55)$$

In this case, the increase in lift force when the aileron deflects is equal to the total decrease in lift force in each section due to the deformation angle.

$$P_{[3]z}(\delta_a) = \Delta P_{[3]z}(\vartheta_{[3]x}) + \Delta P_{[2]z}(\vartheta_{[2]x}) + \Delta P_{[1]z}(\vartheta_{[1]x}) \quad (56)$$

The dependencies can be represented analytically in a fairly simple form. And the change in the increase in lift force due to the deformation of the elastically suspended wing compartment when the aileron is deflected by an angle δ_a is determined by the formula

$$\Delta P_{[i]z}(\vartheta_{[i]x}) = A_{[0,i]} \cdot \vartheta_{[i]x}, i = \overline{1,3} \quad (57)$$

The corresponding deformation angle i of the section is defined as:

$$\mathcal{G}_{[i]x} = S_{[0,i]}^{-1} \cdot M_{[i]x} \quad (58)$$

and $M_{[i]x}$ and $S_{[0,i]}$ are determined according to (21) based on the material presented above

The effectiveness of ailerons at speeds below the critical speed and η_R can be express using the efficiency coefficient, which has the following form:

$$\eta_R = \frac{\Delta P_z^\Sigma(C, A)}{P_{[3]z}(\delta_a)} \cdot 100\% \quad (59)$$

3.4 Simulation of flutter

Flutter refers to the phenomena of dynamic aeroelasticity, where the state of the system is influenced by all three types of forces (elastic, aerodynamic, inertial). Then the block diagram includes all three elements.

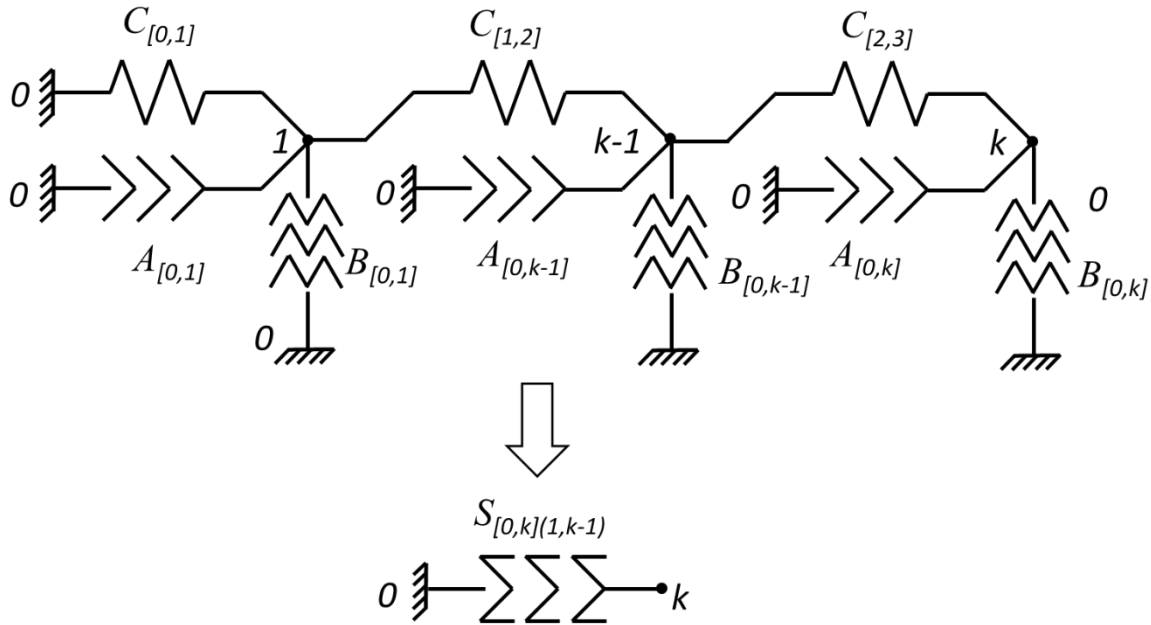


Figure 21: Structural diagram of dynamic phenomena of aeroelasticity.

We transform the diagram to a form with one internodal connection, which is described by the aeroelasticity matrix $S_{[0,k](1..k-1)}$.

$$S_{[k-1,0](1,k-2)} = C_{[k-1,k-2]}(S_{[k-2,0](1,k-3)} + C_{[k-2,k-1]})^{-1}S_{[k-2,0](1,k-3)} + A_{[k-1,0]}, \quad (60)$$

$$S_{[k-2,0](1,k-3)} = C_{[k-2,k-3]}(S_{[k-3,0](1,k-4)} + C_{[k-3,k-2]})^{-1}S_{[k-3,0](1,k-4)} + A_{[k-2,0]} + B_{[k-2,0]} \quad (61)$$

$$S_{[3,0](1,2)} = C_{[3,2]}(S_{[2,0](1)} + C_{[2,3]})^{-1}S_{[2,0](1)} + A_{[3,0]} + B_{[3,0]} \quad (62)$$

$$S_{[2,0](1)} = C_{[2,1]}(S_{[1,0]} + C_{[1,2]})^{-1}S_{[1,0]} + A_{[2,0]} + B_{[2,0]} \quad (63)$$

After setting the determinant of the matrix to zero

$$\det S_{[0,k](1..k-1)} = 0 \quad (64)$$

we obtain a characteristic polynomial of the following form:

$$h_0 + h_1 \cdot \lambda + \dots + h_{n-1} \cdot \lambda^{n-1} + h_n \cdot \lambda^n = 0 \quad (65)$$

where $\lambda = p^2$ and n is calculated as considered DOFs multiplying on count elements k .

The coefficients of the characteristic polynomial h are determined by the components of the matrices C , B and $A(V)$, and characterize the state of the system depending on the ratio of elastic, inertial and aerodynamic forces. It is worth noting that, with constant elastic parameters and conditionally constant inertial characteristics, the main influence on the stability of the wing is exerted by aerodynamic loads depending on the speed of the oncoming flow V .

The study of a system for stability is carried out using various stability criteria.

3.5 MDO

The developed mathematical method offers significant advantages, particularly in their ability to perform Global Sensitivity Analysis since in fact tensor modes which were gotten above are the Global Sensitivity Equation (GSE) [27, 24, 25]. This capability is crucial for multidisciplinary design optimization (MDO) in the field of aeroelasticity, especially during the preliminary design stage of aircraft wings. By creating GSEs, this method enable a comprehensive understanding of the sensitivity of aeroelastic system outputs to various input parameters. This leads to more efficient and accurate optimization processes, facilitating better decision-making and resource allocation early in the design process. The integration of GSE in aeroelastic MDO enhances the ability to address complex, interdependent design challenges, ultimately improving the overall performance and robustness of aircraft wing designs.

4 CONCLUSIONS

In this paper, we have introduced a novel methodology for aeroelasticity modeling, offering a comprehensive framework that includes the general theory and approach, a model for analyzing wing divergence, wing deformation, control surface effectiveness, and flutter analysis. Our method utilizes symbolic operations with Computer Algebra Systems (CAS), facilitating explicit dependencies between design parameters and flight performance. This advancement over traditional numerical methods enables multidisciplinary design optimization (MDO) and the solving of inverse aeroelasticity problems.

Our methodology provides clear, analytical expressions for the relationships between design variables and aeroelastic characteristics, enhancing the understanding of how different parameters affect flight performance. The ability to perform MDO in symbolic form allows for more efficient and integrated optimization processes, accommodating various design disciplines simultaneously. Additionally, solving the inverse aeroelasticity problem aids in determining optimal design parameters to achieve desired aeroelastic performance, which is particularly useful in the early stages of aircraft design.

The symbolic nature of our models makes them suitable for integration with artificial intelligence and machine learning algorithms, potentially leading to advanced predictive analytics and optimization capabilities [26]. Our method can be extended to include Aeroservoelasticity,

analyzing the interactions between aerodynamic forces, structural dynamics, and control systems. The framework can also be adapted for nonlinear aeroelastic analysis, enhancing its applicability to real-world scenarios where linear assumptions may not hold. Furthermore, the methodology is versatile enough to be applied to the analysis of rotor wings or blades, expanding its utility to rotary-wing aircraft and other aerospace structures.

However, the primary constraint of our method lies in its reliance on computer algebra systems for handling tensor operations. This dependence can pose limitations in terms of computational resources and the complexity of the symbolic manipulations required for large-scale problems.

In conclusion, our innovative approach to aeroelasticity modeling offers significant advantages in terms of explicit analytical dependencies, optimization capabilities, and versatility in application. Despite its reliance on advanced computational tools, the method provides a robust framework for improving the preliminary design and analysis of aerospace structures. Future research directions include enhancing the computational efficiency of the method and exploring its integration with advanced AI techniques for even greater optimization potential.

REFERENCES

- [1] Ideen Sadreghighi, “Aircraft Conceptual Design Practices & Case Studies”, CFD Open Series Version 2.55
- [2] Adrien Crovato, Romain Boman¹, Vincent E. Terrapon¹, Grigorios Dimitriadis, Alex P. Prado, Pedro H. Cabral., “Fast Full Potential Based Aerostructural Optimization Calculations For Preliminary Aircraft Design” IFASD, 2022
- [3] Xavier Carrillo Córcoles*, Roeland De Breuker., Jurij Sodja “Aeroelastic Tailoring of Strut-Braced Wings Wing for a Medium Range Aircraft” AIAA SciTech Forum, 2024
- [4] Oriol Chandre-Vila, Jean-Philippe Boin, Bernard Barriety, Yann Nivet, Joseph Morlier, “Fast Nonlinear Method for Static Aeroelasticity Applied to High Aspect Ratio Wings” Journal of Aircraft, 2023, pp.1-21.
- [5] Christian Anhalt, Hans Peter Monner, Elmar Breitbach, “Interdisciplinary Wing Design – Structural Aspects” SAE 2003 Transactions Journal of Aerospace
- [6] Ilan Kroo, Steve Altus, Robert Braun, Peter Gage, and Ian Sobieski “Multidisciplinary optimization methods for aircraft preliminary design” AIAA-94-4325-CP
- [7] Shirk, M. H. and Hertz, T. J. “Aeroelastic Tailoring - Theory, Practise and Promise. Journal of Aircraft”, 1986, 23(1), 6–18.
- [8] L. Cavagna, S. Ricci, L. Riccobene, “A Fast Tool for Structural Sizing, Aeroelastic Analysis and Optimization in Aircraft Conceptual Design”, Structural Dynamics, and Materials conference 17th, 2009, AIAA 2009-2571
- [9] Abdelkader Benaouali, Stanisław Kachel, “Multidisciplinary design optimization of aircraft wing using commercial software integration”, Volume 92, September 2019, Pages 766-776

- [10] Chi Zhang , Zhou Zhou *, Xiaoping Zhu and Lina Qiao, “A Comprehensive Framework for Coupled Nonlinear Aeroelasticity and Flight Dynamics of Highly Flexible Aircrafts”, Applied science, 2020, Volume 10 (3), 949
- [11] Guanghui Shi(&), Yupeng Zhang, Dongliang Quan, Dongtao Wu, Chengqi Guan, “Conceptual Design of Aircraft Structure Based on Topology Optimization Method”, Advances in Structural and Multidisciplinary Optimization, 2017, p 1083–1093
- [12] Henrik Hesse, Rafael Palacios, “Reduced-Order Aeroelastic Models For The Dynamics Of Maneuvering Flexible Aircraft” IFASD, 2013,
- [13] Mikhail Itskov “Tensor Algebra and Tensor Analysis for Engineers” Textbook, 2019
- [14] Peter H. Zipfel, “Introduction to Tensor Flight Dynamics”, Modeling and Simulation Technologies, 2023
- [15] Peter Baranyi, “Tensor Product Model-Based Control of Two-Dimensional Aeroelastic System” Journal Of Guidance, Control, And Dynamics, 2006, Vol. 29, No. 2,
- [16] Béla Takarics, Péter Baranyi, “Tensor-Product-Model-Based Control of a Three Degrees-of-Freedom Aeroelastic Model” Journal Of Guidance, Control, And Dynamics, 2013 Vol. 36, No. 5
- [17] Bela Takarics, Alexandra Szollosi, Balint Vanek, “Tensor Product Type Polytopic LPV Modeling of Aeroelastic Aircraft”, IEEE Aerospace Conference, 2018
- [18] Johan Andersson and Petter Krus, “A Multi-Objective Optimization Approach to Aircraft Preliminary Design”, SAE World Aviation Congress, 2003
- [19] Balabanov I.V., Balabanova T.V, Havaza O.Y. “Methods of calculating the aircraft wing characteristics with influence aeroelasticity” Mechanics of gyroscopic systems, 2015
- [20] Balabanov I.V., Balabanova T.V, Havaza O.Y. “The optimal design of high speed wing aircraft” X International Conference Gyrotechnology, Navigation, Movement Control And Aerospace Technic Engineering, 2015
- [21] John Wiley, Sons, Chichester, “Computer Algebra Systems: A Practical Guide”, Textbook, 1999
- [22] Balabanov I.V., Balabanova T.V. “Nodal method condensation for calculation elastic spatial systems”.Analytical mechanics and its publication: Collection of the Institute of Mathematics of the National Academy of Sciences of Ukraine, 2012,Vol.9 No. 1-P.11-37
- [23] Balabanov I.V., Balabanova T.V, Zbrutskyi A.V. “Calculation and optimization of two frame elastic suspensions of a dynamically adjustable gyroscope”, Monograph, NTUU “KPI”, 2013
- [24] Joaquim R. R. A. Martins “Multidisciplinary design optimization: A survey of architectures” AIAA Journal, 2013, Vol. 51(9):2049–2075

[25] Joaquim R., R. A. Martins, Andrew Ning “Engineering Design Optimization” Textbook 2021

[26] Bo Zhang , Jinglong Han, Haiwei Yun, Xiaomao Chen, “Nonlinear Aeroelastic System Identification Based on Neural Network” Applied science, 2018, Vol. 8(10), 1916

[27] Ideen Sadreghighi, “Aircraft Multidisciplinary Design & Optimization (MDO) Multi-point Optimization of Aircraft Wings using Coupling CSD & CFD”, CFD Open Series Version 2.40,

COPYRIGHT STATEMENT

The authors confirm that they, and/or their company or organisation, hold copyright on all of the original material included in this paper. The authors also confirm that they have obtained permission from the copyright holder of any third-party material included in this paper to publish it as part of their paper. The authors confirm that they give permission, or have obtained permission from the copyright holder of this paper, for the publication and public distribution of this paper as part of the IFASD 2024 proceedings or as individual off-prints from the proceedings.